RSC Advances

ROYAL SOCIETY OF CHEMISTRY

www.rsc.org/advances

Thermal decomposition and desorption of PFPE Zdol on a DLC substrate using quartic bond interaction potential

S K Deb Nath[1]

[1]Computational Materials Research Initiative, Institute for Materials Research, Tohoku University, Japan

Abstract

At heat assisted magnetic recording (HAMR) system heating of the hard disk magnetic layer is carried out by applying laser rays during the movement of the head on the carbon overcoat for the purpose of reading and writing on its magnetic layer. Depletion of PFPE Zdol occurs for the cause of its thermal decomposition and desorption on a DLC substrate due to laser heating and this model is developed using the coarse-grained bead spring based on quartic and Van der Waals interaction potential. Effect of temperature on the bond breaking phenomenon of PFPE Zdol due to thermal decomposition and thermal desorption are studied. To support the reliability of the present simulation results by quartic potential, the end bead density and total bead density on a DLC substrate obtained by the finitely extensible non-linear elastic (FENE) and quartic potential are shown as a comparative manner.

***Keyword*:** Thermal decomposition, thermal desorption, PFPE Zdol, quartic potential

1. Introduction

In MEMS/NEMS, PFPE films are used as permanent lubricant to protect these structures from erosion [1-2]. Hard disk industry uses thin PFPEs (with a thickness of 1-2nm) deposited onto amorphous carbon overcoat to protect underlying hard disks from mechanical damage during intermittent contacts with the read-write heads as the disk rotates. Conventional reading-writing technique to increase the memory of a hard disk has a limitation to reach above 1TB/inch^2. But the only way is heat-assisted magnetic recording technology is the alternative way to reach the memory up to 10 TB/inch^2. But the main difficulties are the stability of lubricants on the hard disk is a great concern to the scientific community. Ganesh et al. [3] showed the successful fabrication of a thin, transparent, and homogenous coating of perfluoropolyether (PFPE) on a smooth glass surface by electro spraying technique. The wetting behavior of three

nanometer thick perfluoropolyether (PFPE) polymers with the same backbone but different end-groups were studied by contact angle tests and simultaneous governing mechanisms like oleophobicity/hydrophilicity were investigated [4]. Li and Wong [5] carried out molecular dynamics simulations to study the thermal stability of thin lubricant films. Lubricant film thickness, bonding ratio, molecular weight and laser heating rate play important roles to deplete lubricant films [6-9]. Wu [8] described a model for lubricant flow dynamics under a scanning laser beam and studied the mechanisms of lubricant on both glass and aluminum disks. The main causes of the depletion of the lubricant film on a hard disk surface are thermal decomposition and desorption but the mechanisms of thermal decomposition and desorption are not understood either by theoretical or experimental way till now [9]. Magnetic layer of a hard disk is heated above its Curie temperature in heat-assisted magnetic recording systems [10]. Pacansky and Waltman [11] reported that PFPEs degrade due to main chain scission when subjected to electron irradiation. Heller et al.[12] investigated the effect of localized laser heating on molecularly thin PFPE lubricants for short times. Zhu et al.[13] used mass spectroscopy to study the thermal chemistry of laser-irradiated PFPEs on disk media. It was found that there is a stronger likelihood of laser-induced scission and rearrangement of the PFPE backbone chain than that of its end group with the laser power density being in a range 60-140 mJ/cm^2. Li et al.[14] employed molecular dynamics (MD) simulation to investigate the evolution and degradation characteristics of ultrathin PFPEs under laser irradiation. They observed that the lubricant diffused radially away from the heating spot and raised ridge was formed around the depleted zone due to non-uniform distribution of surface tension and thermo capillary stress. Waltman and Tyndall [15-16] measured the evaporation rates of both polydisperse and monodisperse PFPEs from a CH_x surface at various temperature. Lim and Gellman [9] investigated the kinetics of laser induced desorption and decomposition of Fomblin Zdol on carbon overcoats. They observed that under HAMR conditions lubricant films with molecular weight of less than 3000 g/mole desorb more than that of decomposition on the disk surface during rapid heating, while decomposition is performed at temperatures (<400^{0}C) expected in HAMR for higher molecular weighs lubricants. The decomposition behavior of Fomblin Zdol and Fomblin Z on amorphous carbon overcoat using thermal desorption spectroscopy [17], the decomposition mechanisms of PFPE Zdol at the head disk interface under sliding conditions [18], desorption mechanisms of Fomblin Zdol on graphite surface [19], thermal stability of Fomblin Z on Al_2O_3 surface [20], thermal decomposition of Fomblin Zdol on graphite and amorphous carbon surfaces [21], thermal and electron-induced decomposition of

Fomblin Zdol on a carbon overcoat [22], the desorption and decomposition of polyperfluorinated ether using transmission infrared spectroscopy [23] were studied experimentally and reported. Lei et al. [17] observed that the decomposition of Fomblin Zdol on amorphous carbon surface occurs in the range of temperature 600-700K and they suggest that desorption is the results of the decomposition of Fomblin Zdol. Kasai et al.[20] observed during the experiment that Fomblin Z on Al_2O_3 surface degrades at 473K at two stages and the vigorous second stage leads to complete loss of fluid. Vurens and Mate [21] concluded from their study on Fombin Zol that the two desorption features of Fomblin Zdol on graphite surface happens at temperatures 620 and 770K; on the other hand the main desorption features of Fomblin Zdol on amorphous carbon surface are at the temperature 510 and 650K.

Tagewa et al. [24-25] carried out a series of experiments to investigate the lubricant depletion characteristics of HAMR systems. They found that the lubricant depletion due to laser heating is largely affected by film thickness, bonding ratio, molecular weight and end groups of lubricant. Ma et al.[26] studied the lubricant depletion on a self-developed HAMR tester and found that the lubricant depletion depth is proportional to the logarithm of laser heating duration. Moreover, they suggested that almost all the lubricant on the disk would be depleted over the lifetime of the hard disk drive. Bei et al.[39] employed molecular dynamics simulation coupled with a course-grained bead-spring polymer model to study the depletion of PFPE lubricants. Their study shows that desorption of PFPE lubricants is favored over decomposition at high temperature. The photo-thermal stability and tribological properties of Zdol lubricant, modified by substituting the OH groups with benzophenone, were investigated using laser beam exposure by Gauvin et al.[27] and they concluded that their modified Zdol lubricant is suitable for heat assistant magnetic recording systems.

From the above study, it is observed that desorption and decomposition rate of functional lubricant film on a thin DLC film using a bond-breaking potential are not available. In the present study we study desorption and decomposition of PFPE Zdol on a thin DLC film considering interaction of all carbon atoms with the lubricant film. New potential quartic is used instead of FENE potential which allows bond-breaking. To satisfy the current results obtained by quartic potential, at low temperature, end bead density and total bead density with the film thickness are computed by using quartic and FENE potential and are compared to each other. To study the validity of the present simulation results, the number density as a function of the film thickness, the

decomposition and desorption rate with the film thickness are compared with the published results. Effects of temperature on the desorption and decomposition rate of PFPE Zdol are investigated in details. With the graphical results, some snapshots during the depletion of lubricants are described to understand the physics of lubricant on a DLC substrate during heating.

2. Simulation details

Figure 1 shows the interaction between the beads of lubricant molecules and DLC substrate. DLC substrate consists of carbon atoms. DLC substrate is prepared subsequent heating and quenching of BCC or FCC diamond crystals by molecular dynamics simulations following the procedures [28-31] using Tersoff potential [32-33]. DLC substrate obtained from atomistic simulation is compressed half of its original dimension so that no lubricant molecules can diffuse inside the DLC substrate during simulation [34-35]. Each lubricant molecule of PFPE Zdol is constructed considering bead spring model. Each beads consists of several PFPE Zdol atoms. Each lubricant molecules consists of 10 beads and among them end beads are considered as polar or functional beads and the rest of the beads are considered as backbone beads. The neighboring beads in each chain are connected by bonds which is modeled using quartic potential and this bond can break anytime if the bond exceeds its allowable extension limit. Practically DLC substrate consists of many dangling bonds and for this reason the functional beads of lubricant molecules are attracted more than the rest of the lubricant molecules [36-37]. Besides, the interaction between the functional beads is more than that of non-functional beads or that of functional and non-functional beads. So for this reason, a special treatment is done between the interaction of functional beads to DLC substrate and among functional beads. The detailed description of the potentials and their interaction are described in the theoretical section using Fig.1.

900 lubricant molecules are considered in the present study. 900 lubricant molecules are kept on a DLC substrate and simulated for long time by the subsequent isothermal heating to obtain the initial configuration of PFPE Zdol film which is shown in Fig.2 [34-35]. After getting an initial configuration of PFPE Zdol film on a DLC substrate, three dimensional simulation is considered considering periodic boundary conditions in x and y directions and in the z direction shrink-wrapped boundary conditions [38] are used because during the simulation the simulation box dimension alters in z direction. Used time step during the simulation 0.005τ. During simulation the positions of carbon atoms in a DLC substrate is kept fixed. Isothermal heating is carried out on the

molecules of PFPE Zdol lubricant molecules on a DLC substrate at different temperature separately. During simulations at high temperature bond breaking happens and new short chains are generated which enhance the thermal decomposition and desorption. The simulations are carried out separately at different isothermal heating for 2000,000 steps for example T*=1 to 6 using NVT (N=same number of atoms, V=volume, T=temperature) canonical ensemble, and we calculate how many bonds break and how many lubricant molecules washed away by desorption phenomenon during the simulation at specific temperature at last time step. Besides, gradual heating effects are also considered heating the lubricant molecules from T*=1 to 6 at slow rate at time step 2000,000 using the NVT canonical ensemble at the same simulation. The simulation is rescaled at every 20 steps. Thermal decomposition and thermal desorption of PFPE Zdol on a DLC substrate is calculated for each case at a time step 2000,000. To verify the soundness of the present simulation results, PFPE Zdol lubricant molecules on a DLC substrate is simulated using FENE and Quartic potentials for bonding between beads of PFPE Zdol molecules, separately keeping the other potential parameter same at a very low temperature T*=1.3.

3. Theories of functional lubricant on a thin DLC film

To describe the bond interaction between the neighboring beads in each lubricant molecule, FENE potential [39-40] is used in the coarse-grained bead spring model. As the FENE potential is unable to bond breakage during the simulation, quartic potential [41-42] is used instead of FENE potential [39-40].

$$U_4 - \begin{cases} k_4(y-b_1)(y-b_2)y^2 + U_0 & r < r_b \\ U_0 & r > r_b \end{cases} \qquad (1)$$

Where r is the distance between two neighboring beads, $y = r\text{-}r_b$ shifts the quartic center from the origin and r_b is the cutoff length where the potential goes smoothly to a local maximum. When the bond breaks and the quartic term is deactivated to impede the bond from reforming. This potential mimics the FENE potential by setting the following parameters as

$k_4 = 1434.3\varepsilon/\sigma^4$, $b_1 = -0.7589\sigma$, $b_2 = 0.0$, $r_b = 1.5\sigma$, and $U_0 = 67.223\varepsilon$ [43-44]

The expression of non-bonded potential LJ 12/6 is

$$U_{LJ12/6} = 4\varepsilon\left[\left(\frac{\sigma}{r}\right)^{12} - \left(\frac{\sigma}{r}\right)^{6}\right] \quad (2)$$

Here σ is the L-J diameter of the beads and ε is the potential depth.

The equation (2) is used for the interaction between non-functional beads; nonfunctional bead to functional bead of PFPE Zdol. As dangling bonds in the DLC film are available, polar beads attract toward the DLC surface to form bond with hydrogen from their OH group and form an ionic bond with the DLC surface. Therefore, an extra attractive potential is added with the van der Waals interactions to satisfy the conditions [44]. For the extra interaction due to the functional effects of the end beads of functional lubricant PFPE Zdol [34-35, 39-40, 44] used expression of the extra interaction between them by an exponential potential is

$$U_{\mathrm{EXP1}} = -\boldsymbol{\varepsilon}_{\mathrm{p}}\left(-\frac{r - r_{\mathrm{c}}}{d}\right) \quad (3)$$

For the extra interaction due to the functional effects of the end beads of functional lubricant PFPE Zdol and DLC C atom [34-35,39-40,44] used expression of the extra interaction between them by an exponential potential is

$$U_{\mathbf{EXP2}} = -\boldsymbol{\varepsilon}_{\mathrm{p}}^{\mathrm{dlc}}\left(-\frac{r - r_{\mathrm{c}}}{d}\right) \quad (4)$$

Combining non-bonded potential LJ 12/6 and exponential potential for the interaction between the end beads of functional lubricant PFPE Zdol, the expression of the resultant energy between polar end bead to polar end bead [34-35, 39-40,44] is

$$U_{\mathrm{eb-eb}} = U_{\mathbf{LJ12/6}} + U_{\mathbf{EXP1}} = 4\boldsymbol{\varepsilon}\left[\left(\frac{\sigma}{r}\right)^{12} - \left(\frac{\sigma}{r}\right)^{6}\right] - \boldsymbol{\varepsilon}_{\mathrm{p}}\left(-\frac{r - r_{\mathrm{c}}}{d}\right) \quad (5)$$

Combining the non-bonded potential LJ 12/6 and exponential potential for the interaction between the end beads to DLC C atoms, the expression of the resultant energy between polar end bead and DLC C atom [34-35, 39-40,44] is

$$U_{\text{eb-dlc}} = U_{\text{LJ12/6}} + U_{\text{EXP2}} = 4\varepsilon\left[\left(\frac{\sigma}{r}\right)^{12} - \left(\frac{\sigma}{r}\right)^{6}\right] - \varepsilon_p^{dlc}\left(-\frac{r - r_c}{d}\right) \quad (6)$$

The detailed descriptions of the parameters in the above equations are given in the reference [34-35, 39-40, and 44-45].

4. Results and Discussion

From the experimental studies it is observed that depletion of PFPE Zdol lubricant on a DLC substrate occurs at high temperature. The reason of the depletion of PFPE Zdol on a DLC substrate is not clear till now. For this reason, theoretical analysis of the depletion of PFPE Zdol on a DLC substrate is necessary to understand the actual physics and chemistry of PFPE Zdol on a DLC substrate at low to high temperature. Two main reasons of the depletion of PFPE Zdol on a DLC substrate are assumed which are thermal decomposition and thermal desorption. Generally static, kinetic and rheological properties of PFPE Zdol on a DLC substrate can be investigated using coarse-grained bead spring model based on FENE potential but it can not be applied at higher temperature because at higher temperature lubricant bond breaks due to increased its bond length. So for this reason, coarse-grained bead spring model based on quartic potential which allows bond breaking during the simulation at higher temperature. As at a low temperature, T* =1.3, PFPE Zdol on a DLC substrate is studied using two different potentials such as quartic and FENE keeping the same Van der Waals interaction and extra attractive potential to verify the reliability of quartic potential on the coarse-grained bead spring model. Figure 3(a) illustrates the end bead density of PFPE Zdol on a DLC substrate as a function of film thickness using two different potentials such as quartic and FENE based on coarse-grained bead spring models. Two layers of PFPE Zdol on a DLC films are formed in which the first peak of the end bead density of PFPE Zdol is largely higher than that of second peak for the case of both potentials. In the 1st layer, the end bead density of PFPE Zdol using quartic potential is slightly smaller than that of FENE potential but except the first layer, the end bead density of PFPE Zdol for the cases of both potentials coincide each other. Figure 3(b) illustrates the total bead density of PFPE Zdol on a DLC substrate using two different potentials such as quartic and FENE as a comparative manner. The first peak of the total bead density of PFPE Zdol using quartic potential is higher than that of the

first peak of FENE potential but except the first peak, the total bead density of PFPE Zdol on a DLC substrate for both of the potentials are almost same with film thickness. From Figs.3 (a) and 3(b), it is clearly observed that the phase transition of PFPE Zdol originates between the first and second layers. Figure 4 shows the comparative study of number density of PFPE Zdol on a DLC substrate as a function of the film thickness using quartic potential based coarse-grained bead spring model with that of PFPE on a single wall obtained by Bei et al., 2013. The obtained number density of PFPE Zdol on a DLC substrate by us qualitatively agree well with that of Bei et al., 2013 and some discrepancies of our result with that of Bei et al., 2013 occurs because Bei et al., 2013 used non-functional PFPE lubricant instead of functional PFPF Zdol and single wall instead of DLC substrate in their simulations. Figure 5 illustrates the total bead density of PFPE Zdol on a DLC substrate at higher temperature such as T*=3.1, 3.4, 3.5 and 3.9. From the this figure, a clear phase transition zone of PFPE Zdol is observed where the liquid phase of PFPE Zdol transforms into a gaseous phase. Besides, from this figure, it is clear that with the increase of temperature, the total bead density not only decreases with the film thickness but also the film thickness of PFPE Zdol on a DLC substrate decreases with the increase of temperature. From figure 5, it is evident that heating of PFPE Zdol on a DLC substrate at a higher temperature is responsible for higher lub depletion than the heating of PFPE Zdol at lower temperature. Figure 6(a) shows the initial configuration of PFPE Zdol on a DLC film at a temperature T*=3 at time step=0. Figure 6(b) shows the final configuration of PFPE Zdol on a DLC substrate during isothermal heating at time =10000τ. After time 10000τ due to isothermal heating, the film of PFPE Zdol on a DLC substrate deplete which are clearly observed if is compared the snapshots of PFPE Zdol on a DLC substrate as observed in Fig.6(a) and 6(b). At time 10000τ, it is observed that in few spots on the DLC substrate, PFPE Zdol lubricant is removed due to isothermal heating at temperature T* =4.0.

Figure 7 illustrates the comparative study of the bond percentage of PFPE Zdol on a DLC substrate with that of non-functional PFPE on a single wall obtained by Bei et al., 2013. Up to temperature T*=4, the bond percentage of PFPE Zdol on a DLC substrate by us quantitatively agree well with that of non-functional PFPE on a single wall obtained by Bei et al., 2013 but the deviation between the bond percentage of PFPE Zdol on a DLC substrate and non-functional lubricant PFPE on a single wall obtained by Bei et al., 2013 increases after temperature T*=4 with the increase of temperature because functionality of PFPE Zdol lubricants and DLC substrate play an important role such types of deviation from that of Bei et al., 2013. For the case of PFPE Zdol

lubricants, functional beads form strong bond with the DLC substrate. As the non-functional PFPE has no functional beads, they cannot form strong bond with the carbon overcoat. For this reason, at the high temperature the decomposition rate of PFPE Zdol should be lower than that of non-functional PFPE lubricants and this effect is strongly observed in the comparative study as shown in Fig.7. Figure 8(a) illustrates the bond percentage of PFPE Zdol on a DLC substrate for the temperature range T* =1.5 to 4. Figure 8(b) illustrates the bond percentage of PFPE Zdol on a DLC substrate as a function of elapsed time during the simulation at the temperature range T*=4 to 6. From Fig.8(a), at the temperature T* =1.5, the bond percentage of PFPE Zdol is nearly 100%, which means that bond of PFPE Zdol on a DLC substrate does not break which ensures that at T*=1.5, no thermal decomposition of PFPE Zdol on a DLC substrate happens at this temperature during the simulation. From Fig.8(a), it is observed that at temperature T* =2, the total bond percentage of PFPE Zdol on a DLC substrate is very high as compared to temperature T* =3, i.e. at temperature T* =2, the rate of bond breaking phenomenon is extremely lower as compared to higher temperature T* =3 or other temperatures. From Figure 8(a) and 8(b), it is evident that with the increase of temperature, bond percentage of PFPE Zdol on a DLC substrate decrease which means the increased temperature enhances the bond breaking phenomenon of PFPE Zdol on a DLC substrate which also increases the thermal decomposition of PFPE Zdol on a DLC substrate. After elapsed time 1000τ, the rate of bond percentage with time during the simulation gradually decreases as before because after elapsed time 1000τ, many beads of PFPE Zdol lubricant exceeds their force cut off distance and many short chains form after 1000τ, the percentage of long chain decreases and for which the increasing rate of bond breaking decreases in the range of elapsed time 1000τ to 10000τ.

To validate the result of thermal desorption of PFPE Zdol on a DLC substrate obtained by us is compared with that of non-functional PFPE lubricant on a single wall obtained by Bei et al., 2013 at two different temperatures such as T*=3 and 3.3 as shown Fig.9. For the case of temperature T*=3, it is observed that weight percentage of PFPE Zdol on a DLC substrate by us agree well qualitatively with that of non-functional PFPE on a single wall obtained by Bei et al., 2013 but at T*=3.3, the deviation of the weight percentage of PFPE Zdol on a DLC substrate obtained by us and the weight percentage of non-functional PFPE on a single wall obtained by Bei et al., 2013 is quietly larger as compared to temperature T*=3 due to the functionality of PFPE Zdol and DLC substrate. Figure 10(a) illustrates the weight percentage of PFPE Zdol on a DLC substrate as a function of elapsed time for the temperature range T* =1.5 to 4. Figure

10(b) illustrates the weight percentage of PFPE Zdol on a DLC substrate as a function of elapsed time for the temperature range T* =4 to 6. At temperature T* =1.5 and 2, the bond percentage of PFPE Zdol on a DLC substrate as a function of elapsed time decreases at constant rate. At temperature T* =1.5, the thermal desorption of PFPE Zdol is very low which can be negligible because at elapsed time, the weight percentage of PFPE Zdol on a DLC substrate is close to 100%. With the increase of temperature, the weight percentage of PFPE Zdol on a DLC substrate decreases. The desorption rate of PFPE Zdol is several times of thermal decomposition during heating PFPE Zdol on a DLC substrate. Up to elapsed time 1000τ, the desorption rate of PFPE Zdol on a DLC substrate is constant and higher than that of rest of the elapsed time. Thermal decomposition enhances the thermal desorption of PFPE Zdol because during heating many small lubricant chain forms due to bond breaking which increases the thermal desorption. Figure 11(a) illustrates the initial configuration of PFPE Zdol on a DLC substrate which is heated at varying temperature T* =1-6 during elapsed time 10000τ as observed in Fig. 11. At the final stage, most of the PFPE Zdol molecules are washed away from the DLC substrate due to having higher temperature T* =6 when it reaches at final stage of heating time 10000τ as shown in Fig.11(b). Some lubricant molecules are attached on the DLC substrate which form strong bond on the DLC substrate. PFPE Zdol lubricant molecules on the DLC substrate form strong bond and are strongly bonded with the DLC substrate and the lubricant molecules on the top surface of lubricant film are non-bonded. During heating, the kinetic energy of each bead increases and for this reason, the bond length increases with the rise of temperature during heating. When the bond length exceeds its allowable limit, bond breaks and new short chains appear on the film. During heating at high temperature, non-bonded lubricants are removed rapidly by desorption and the PFPE Zdol thickness decreases. As the lubricant on the DLC substrate form strong bond with the DLC substrate, all lubricant molecules are not washed away from the DLC substrate as shown in Fig.11 (b). Bond percentage of PFPE Zdol on a DLC substrate is also studied in two different cases as shown in Figs.12(a) and 12(b) such as in the first case, bond percentage of PFPE Zdol is studied as a function of elapsed time during heating temperature T* =1-6 as shown in Fig.12(a). In the second case, bond percentage of PFPE Zdol is studied as a function of temperature T* during heating up to elapsed time 10000τ as shown in Fig.12 (b). During heating of PFPE Zdol on a DLC substrate, bond percentage of PFPE Zdol decrease at a very low constant rate up to temperature T*=1 to 3 or up to elapsed time upto 4000τ during the simulation. After reaching temperature T* =3 or elapsed time 4000τ, the decreasing rate of bond percentage of PFPE Zdol on a DLC substrate

increases upto T* =5 or elapsed time 7000τ and after reaching temperature T* =5 or elapsed time 7000τ , the bond percentage of PFPE Zdol on a DLC substrate increases at a constant rate to reach the final stage at time 10000τ or temperature T* =6. Thermal decomposition of PFPE Zdol is dominating in the temperature range T*=4 to6 which agree well qualitatively with that of the experimental study of the thermal decomposition of Fomblin Zdol on a carbon surface by Lei et al.[17]. In the theoretical study of non-functional PFPE lubricants [39] and the experimental study of Fomblin Zdol on a carbon surface favors desorption over decomposition. And the similar effects are also observed in our study and from present study of thermal decomposition and desorption of PFPE Zdol on a DLC substrate, desorption of PFPE Zdol favors over the decomposition.

5. Conclusion

From the comparative study of the end bead density and total bead density of PFPE Zdol on a DLC substrate at a temperature T* =1.3 obtained by quartic potential and FENE potential agree well each other. But at higher temperature bond breaking phenomenon happens which cannot be solved using FENE potential but quartic potential allows bond breaking phenomenon during heating at high temperature. From the total bead density of PFPE Zdol using quartic potential, clear phase transition zone is observed in where liquid PFPE Zdol turns into gaseous phase. With the increase of temperature, thermal decomposition and thermal desorption of PFPE Zdol on a DLC substrate increases. Thermal desorption is the principle cause of lub desorption. But due to thermal decomposition, many long lubricant chain turn into short chains which enhance thermal desorption of PFPE Zdol lubricant molecules on a DLC substrate.

References

1. B.Marchon, *IEEE Trans. Magn*., 2009, **45**,872-876.
2. Z. Tao and Bhusan, *Wear*, 2015, **259**,1352-1361.
3.V.A.Ganesh, S.S.Dinachali, S.Jayaraman, R.Sridhar, H.K.Raut, A.Góra, A.Baji, A.S.Nair and S.Ramakrishna, *RSC Advances*, 2014, **4**,55263-55270.
4.Y.Wang,J.Knapp,A. Legere,J.Raney and L.Li, RSC Advances,2015,5,30570-30576
5. B. Li and C.H.Wong, *Computational Materials Science*, 2014, **93**, 11-14.
6. N. Tagawa, H. Andoh and H. Tani, *Tribology Letters*, 2010, **37**,411-418.

7. N.Tagawa, T.Miki and H.Tani, *Tribology Letters*, 2012, **47**,123-129.
8. L.Wu, Nanotechnology, (2007), 18, 215702.
9. M.S.Lim and A,J.Gellman, *Tribology International*, 2005, **38**,554-561.
10.W.A.Challener, C.Peng, A.V.Itagi, D.Karns, W.Peng, Y.Peng,X.Yang,X.Zhu,N.J.Gokemeijer,Y.-T.Hsia,G.Ju,R.E.Rottmayer,M.A.Seigler and E.C.Gage, *Nature Photonics*, 2009, **3** ,220-224.
11. J.Pacansky and R.J.Waltman, *Chem. Mater.* 1993, **5**,486-494.
12.J.Hellor, C.M.Mate, C.C.Poon and A.C.Tan, *Langmuir*, 1991, **15**,8282-8287.
13. L.Zha,T.Liew and T.C.Chang, *Applied Physics A*, 2002,**75**,633-636.
14. Y.Li, C.H.Wong,B.Li, S.K.Yu, W.Hua, and W. Zhou, *Soft Matter*, 2012, 8,5649-5657.
15. R.J.Waltman, G.W.Tyndall, J.Pacansky and R.J.Berry, *Tribology Letters*, 1999, **7**,91-102.
16. G.W.Tyndall, and R.J.Waltman, *J.Phys.Chem. B*., 2000, **104**,7085-7095.
17.R.Z.Lei, A.J.Gellman and P. Jones, *Tribology Letters*, 2001, **11**,1-5.
18. J.Wei, W.Fong, D.B.Bogy and C.S.Bhatia, *Tribology Letters*, 1998, **5**,203-209.
19.K.R.Paserba and A.J.Gellman, *J.Phys.Chem B*, 2001,**105**,12105-12110.
20.P.H.Kasai, W.T.Tang and P.Wheeler, *Applied Surface Science*,1991,**51**,201-211.
21.G.H.Vurens and C.M.Mate, *Applied Surface Science*,1992,**59**,281-287.
22.J-L. Lin, C.S. Bhatia and J.T.Yates, Jr, *Journal of Vacuum Science & Technology A*, 1995,**13**,163-168.
23.L.M.Ng, E.Lyth, M.V.Zeller and D.L.Boyd, *Langmuir*,1995,**11**,127-135.
24.N. Tagawa, R.Kakitani, H. Tani, N.Iketani and I.Nakano, *IEEE Trans. Magn.*,2009,**45**,877-882.
25.N.Tagawa and H. Tani, *IEEE Trans. Magn*., 2011,**47**,105-110.
26.Y.S.Ma, X.Y.Chen and B.Liu, *Tribology Letters*, 2012,**47**,175-182.
27.M.Gauvin, H.Zhang, B.Suen, J.Lee, H.J.Kang and F.E.Talke, *IEEE Transactions on Magnetics* ,2011,**47**,1849-1854.
28.H.Lan, T.Kato and C.Liu, *Tribology International*, 2011,**44**,1329-1332.
29.Z.D.Sha, P.S.Branicio, V.Sorkin, Q. X. Pei and Y.W.Zhang, *Diamond & Related Materials*, 2011,**20**,1303-1309.
30.J.F.Ziegler, M.D.Ziegler and J.P.Biersack, *Nuclear Instruments and Methods in Physics Research B*,2010,**268**,1818-1823.
31.I.N. Remediakis, G.Kopidakis and P.C.Kelires, *Acta Materialia*, 2008,**56**,5340-5344.
32.J. Tersoff, *Physical Review B*,1988,**39**,5566-5568.
33.J.Tersoff, *Physical Review Letters*,1988,**61**,2879-2882.

34.S.K. Deb Nath., C.H. Wong, V. Sorkin, Z.D. Sha, Y.W. Zhang and S.-G. Kim, *Tribology Transactions*, 2013,**56**,255-267.
35.S.K. Deb Nath, *Applied Physics* A, 2014,**117**,857-870.
36.P.H.Kasai, A.Wass and B.K.Yen, J*ournal of Information Storage and Processing Systems*,1999,**1**,245-258.
37.P.H.Kansai and A.M.Spool, *IEEE Transactions on Magnetics*, 2001,**37**,929-933.
38.S.J. Plimpton, *Journal of Computational Physics*, 1995,**117**,1-19.
39.L.Bei, C.H.Wong and Q.Chen, *Soft Matter*, 2013, **9**,700-708.
40.Q. GuO, S. Izumisawa, D.M. Phillips and M.S. Jhon, *Journal of Applied Physics*, 2003,**93**,8707-8709.
41.M.Tsige and M.J.Stevens, Macromolecules,2004,**37**,630-637.
42.M.J.Stevens, Macromolecules, 2001,**34**,1411-1415.
43.S. Izumisawa and M.S. Jhon, *Journal of Applied Physics*, 2002,**91**,7583-7585.
44.P.S. Chung, H. Park and M.S. Jhon, *IEEE Transactions on Magnetics* ,2009,**45**,3644-3647.
45.X. Li, Y. Hu, L. Jiang and J. Zhang, *The Journal of Chemical Physics*, 2008,**128**,194904.

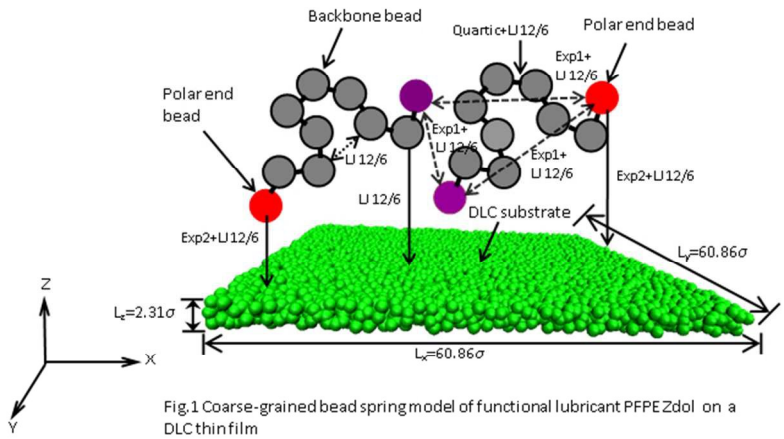

Fig.1 Coarse-grained bead spring model of functional lubricant PFPE Zdol on a DLC thin film

216x121mm (96 x 96 DPI)

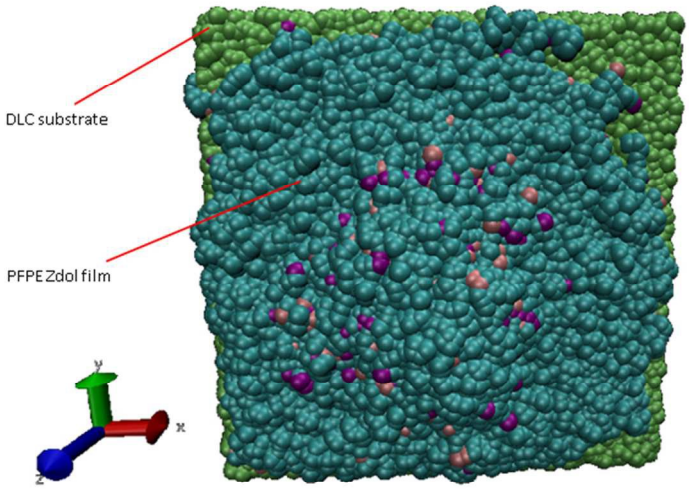

Fig. 2 Front view of initial configuration of PFPE Zdol film on a DLC substrate

216x129mm (96 x 96 DPI)

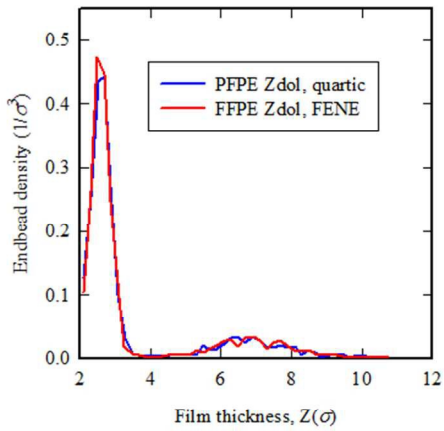

3(a)

216x121mm (96 x 96 DPI)

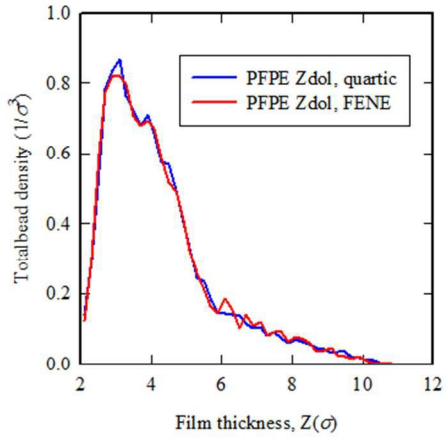

3(b)

Fig.3 Effects of two different potentials such as quartic and FENE :(a) on the film thickness as a function of end bead density; (b) film thickness as a function of total bead density of PFPE Zdol lubricant molecules on a DLC film at a temperature, T* =1.3

216x134mm (96 x 96 DPI)

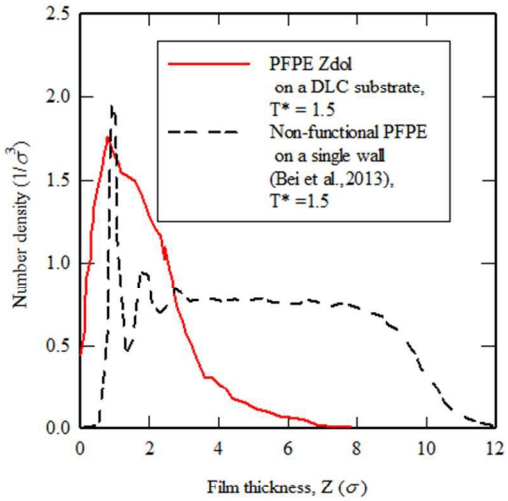

Fig. 4 Comparative study of the number density of beads of PFPE Zdol on a DLC substrate with that of non-functional PFPE on a single wall (Bei et al., 2013) at a reduced temperature T* =1.3

216x129mm (96 x 96 DPI)

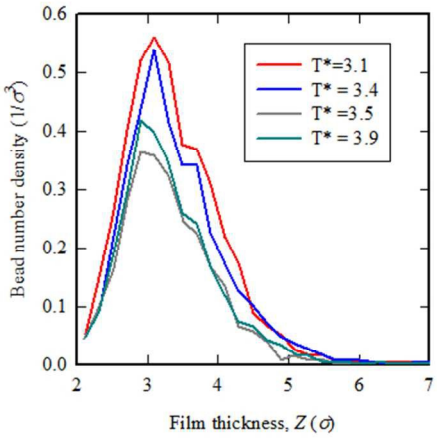

Fig.5 Effect of temperature on the total bead density of PFPE Zdol lubricant as a function of film thickness at temperature T*=3.1, 3.4, 3.5, 3.9

216x129mm (96 x 96 DPI)

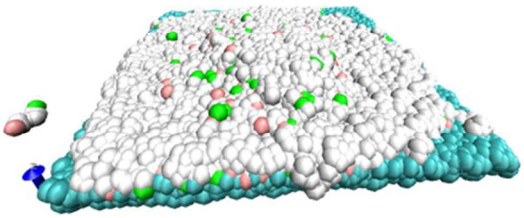

6(a)

216x129mm (96 x 96 DPI)

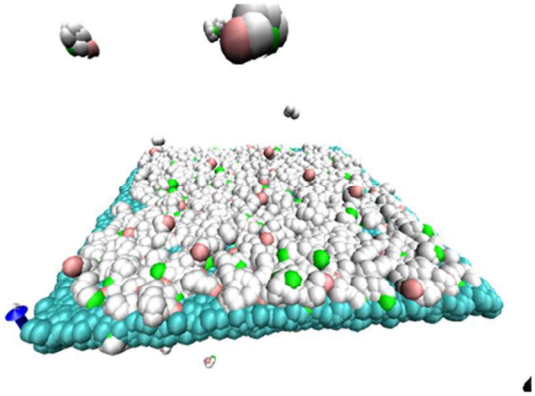

6(b)

Fig.6 Snapshots of PFPE Zdol lubricant molecules on a DLC substrate at constant temperature, T*=3: (a) at time, τ=0; (b) at τ=10000 during isothermal heating

216x129mm (96 x 96 DPI)

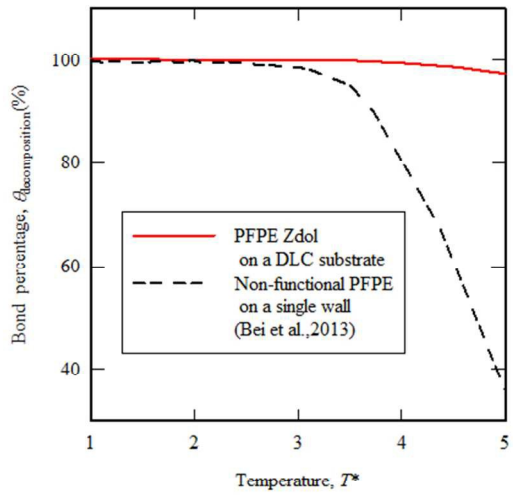

Fig. 7 Comparative study of bond change of PFPE Zdol on a DLC substrate with that of non-functional PFPE on a single wall (Bei et al., 2013) with reduced temperature

216x138mm (96 x 96 DPI)

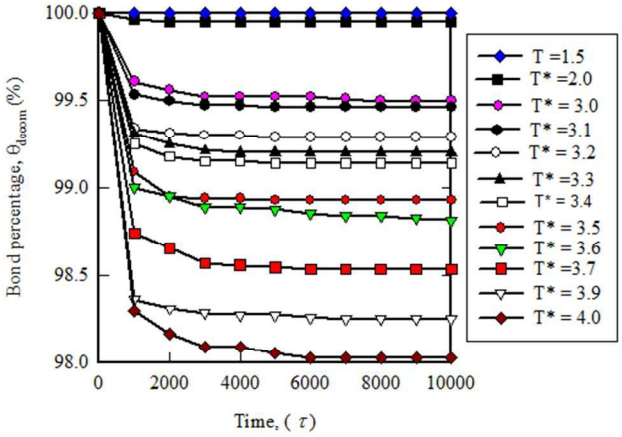

8(a)

216x138mm (96 x 96 DPI)

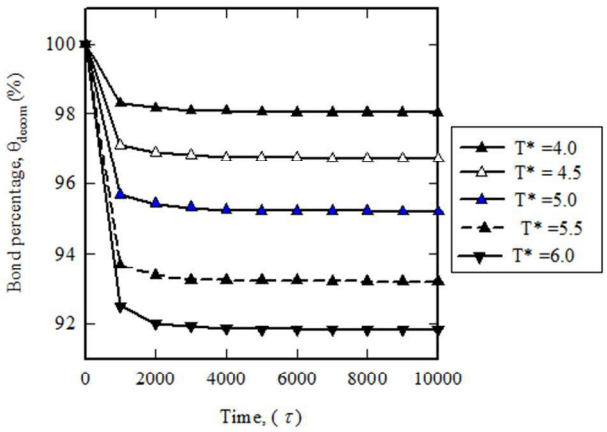

8(b)

Fig.8 Effect of temperature on the bond percentage of PFPE Zdol lubricant molecules on a DLC substrate: (a) at temperature range, T*= 1.5 -4; (b) at temperature range, T*=4-6

216x138mm (96 x 96 DPI)

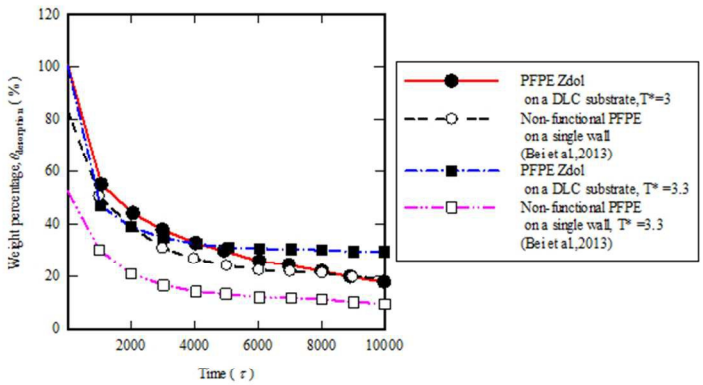

Fig.9 Comparative study of mass change of PFPE Zdol on a DLC substrate with that of non-functional PFPE on a single wall (Bei et al., 2013) with time t

216x138mm (96 x 96 DPI)

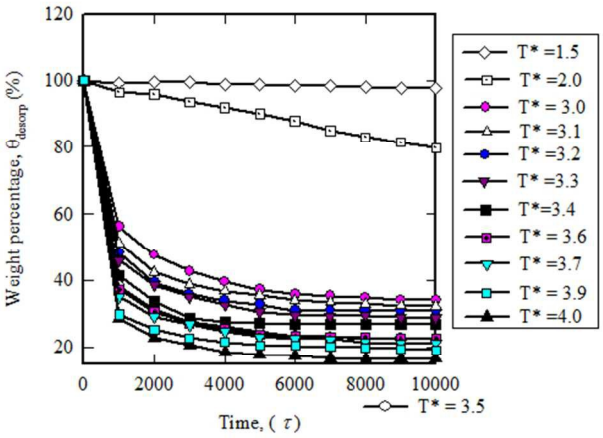

10(a)

216x138mm (96 x 96 DPI)

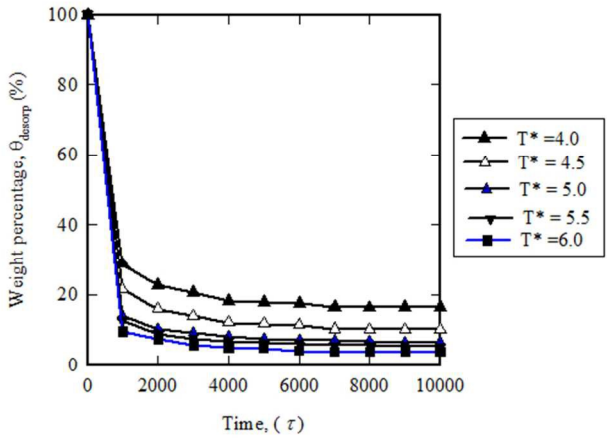

10(b)

Fig.10 Effect of temperature on the weight percentage of PFPE Zdol lubricant molecules on a DLC substrate: (a) at temperature range, T*= 1.5 -4; (b) at temperature range, T* =4-6

216x133mm (96 x 96 DPI)

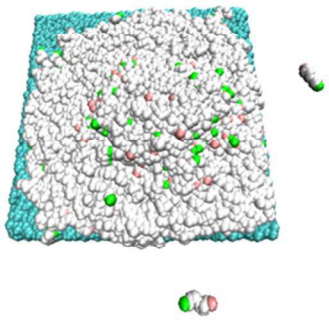

11(a)

216x138mm (96 x 96 DPI)

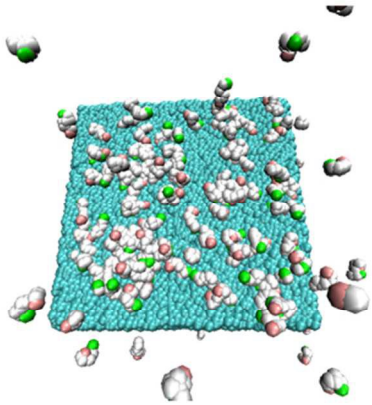

11(b)

Fig.11 Snapshots of PFPE Zdol lubricant molecules on a DLC substrate at varying temperature temperature, T*=1-6: (a) at time, τ=0; (b) at τ=10000

216x138mm (96 x 96 DPI)

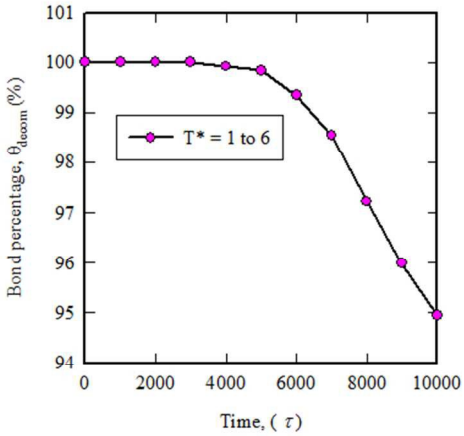

12(a)

216x138mm (96 x 96 DPI)

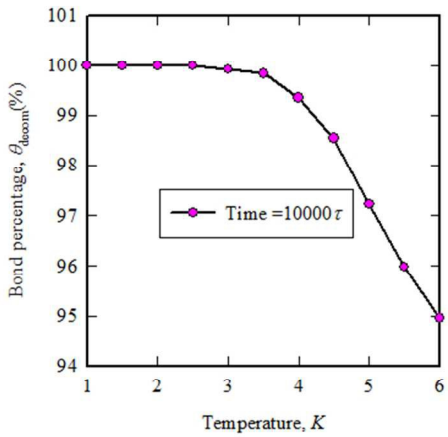

12(b)

Fig.12 Bond percentage of PFPE Zdol lubricant molecules on a DLC substrate: (a) as a function of elapsed time; (b) as a function of temperature during heating at increased temperature T*=1 to 6

216x138mm (96 x 96 DPI)